

# Interfacial Structure of Phosphorylcholine Incorporated Biocompatible Polymer Films

Y. Tang, T. J. Su, J. Armstrong, and J. R. Lu\*

*Biological Physics Group, Department of Physics, UMIST, Manchester M60 1QD, UK*

A. L. Lewis, T. A. Vick, and P. W. Stratford

*Biocompatibles Ltd., Farnham Business Park, Farnham, Surrey GU9 8QL, UK*

R. K. Heenan and J. Penfold

*ISIS Neutron Facility, CCLRC, Rutherford Appleton Laboratory, Chilton, Didcot OX11 1QX, UK*

*Received May 16, 2003; Revised Manuscript Received August 23, 2003*

**ABSTRACT:** Neutron reflectivity (NR) has been used to determine the structure of dry and swollen PC100B biocompatible phosphorylcholine (PC) polymer films coated on the optically flat silicon oxide surfaces. Deuterium labeling to the dodecyl chain of PC100B polymer was found to be effective at highlighting the interfacial structure of dry PC100B films while the swelling with D<sub>2</sub>O into the fully hydrogenated PC100B polymer produced sufficient isotopic contrast for revealing structural features within the swollen films. The main structural characteristics of the dry PC films were found to consist of alternate layers at the SiO<sub>2</sub>/polymer and polymer/air interfaces, indicating that thermal annealing promoted segregation of hydrophilic and hydrophobic moieties within the polymer. The thicknesses of these sublayers were between 10 and 30 Å, and the layering feature gradually became diminished into the middle film region which is characterized by a uniform scattering length density (SLD) determined by NR. It was further observed that the outer surfaces of the dry polymer films contained a significant fraction of hydrophobic moiety as a result of surface energy minimization during annealing, but upon swelling in water this structural feature was deteriorated by fragment motions and redistributions. In contrast to the greater structural variation on the outer film surface, swelling had relatively less effect on the internal layering structure at the SiO<sub>2</sub>/polymer interface due to the structural constraints imposed by silyl cross-linking and the hydrophobic barrier to water diffusion. The thickness of the middle part of uniform region increases with dry film thickness, but the alternate layering at the interfaces was largely unaffected. The increase in annealing temperature enhanced silyl cross-linking, resulting in the reduced equilibrium water content across the films and the slowdown of the rate of swelling.

## Introduction

In this work we report our recent study on the use of neutron reflectivity to determine the structural characteristics of thin phosphorylcholine (PC) incorporated polymer films before and after immersion in aqueous solution. PC polymer coated surfaces are well-known for reducing protein adsorption and for improving surface biocompatibility in biological environment. Biocompatible and bioinert surfaces are receiving increasing attention in the current pursuit of biomaterials development. Applications of biocompatible polymeric materials include biosensors, contact lenses, prostheses, and vascular stents.<sup>1,2</sup> Understanding the molecular mechanistic processes underlying surface biocompatibility is also important for the development of smart materials for micropatterning, bionanotechnology, and tissue engineering.<sup>3–12</sup>

We have previously utilized neutron reflectivity (NR) to probe structural conformations of proteins at the solid/aqueous interface.<sup>13–16</sup> The different extent of structural deformation and unfolding of protein molecules as revealed by NR has clearly indicated the role of surface chemistry on protein adsorption. For example, proteins adsorbed on PC polymer surfaces were found

to be loose packed but broadly distributed. This structural feature was in strong contrast to the narrow and dense protein layer distributions formed on more conventional surfaces such as bare silicon oxide, C18 hydrophobed (end grafted octadecyl chains, OTS) silicon oxide, self-assembled C<sub>15</sub>OH, and poly(methyl methacrylate) (PMMA),<sup>17–22</sup> representing a range of different surface chemistry. Neutron reflectivity thus offers a strong prospect to correlate the surface chemical nature to the in situ conformational structure of the protein and its bioactivity.

The PC polymers used for film coatings contain hydrophilic and hydrophobic moieties, and upon exposure to aqueous solution, the films will swell.<sup>23,24</sup> Swelling could cause interfacial partitioning, resulting in the interfacial composition on the outer surface to be substantially different from the mean polymer composition. This situation makes it difficult to link protein adsorption behavior to the true chemical nature of the polymeric interface. A further important issue is that the extent of PC polymer film swelling is strongly affected by annealing temperature.<sup>23,24</sup> The aim of this work is to determine the interfacial composition of dry and swollen films so that the extent of variation of interfacial composition at the outer surfaces of the polymeric films could be better related to their antiadsorption performance.

\* To whom correspondence should be addressed: e-mail j.lu@umist.ac.uk; Tel 44-161-2003926.

Phosphorylcholine is the zwitterionic lipid headgroup on the outer surface of cell membrane bilayers, and their main role is to prevent cell surfaces from being fouled in the bloodstream. Recent research has shown that polymers incorporating PC groups have inherited the distinct hemocompatibility and biocompatibility.<sup>25–28</sup> A characteristic feature of PC polymer coatings in many biomedical applications is the ultrathin film thickness coupled with a high degree of uniformity. The thickness of the dry films is typically of the order of a few hundred angstroms. This film dimension makes it difficult to follow the kinetic process of film swelling using common methods such as DSC and gravimetric approach. We have recently shown that spectroscopic ellipsometry (SE) offers a fast and effective route to the in situ determination of change of film thickness and water content with time.<sup>23,24</sup> However, because SE measures the variation of the total refractive index across the interface, it has little sensitivity to the structural details within the film. Neutron reflection has been shown to be a much more powerful and accurate technique for providing detailed information on polymer structure,<sup>29,30</sup> especially at the surface and interface of polymer film matrix.<sup>29,31</sup> Also, neutron reflection has been successfully used to illustrate the distributions of small solvent molecules within swollen polymer films.<sup>32–34</sup> The sensitivity of neutron reflection in these applications hinges on two distinct characteristics. First, the wavelength of neutron sources is typically 1–10 Å as compared with a few thousand angstroms in light sources. This makes neutron reflection inherently more sensitive to the structural details at the molecular level. Second, neutron reflectivity is sensitive to the neutron refractive index profile (commonly termed scattering length density, SLD), which varies substantially between hydrogen and deuterium. Thus, deuterium labeling offers an effective means for highlighting structural profiles across polymer films.

Isotopic labeling has been exploited in this work by selective deuteration of the dodecyl chains in the polymer. It was expected that upon annealing segregation between hydrophobic and hydrophilic moieties would occur, leading to the formation of lamellar structure across the PC film. Partial deuterium labeling to the dodecyl chains served to highlight the hydrophobic regions inside the dry film when characterized at the air/solid interface, while the penetration of D<sub>2</sub>O into the fully hydrogenated polymer was effective for highlighting the structural inhomogeneity across the PC film under water. These isotopic labeling schemes have been used to characterize the interfacial structural features of dry and swollen films. The results show the formation of layered structure at both substrate/polymer and polymer/air interfaces under the dry state. Upon swelling, however, the layered structure of the outer film surface was deteriorated by the fragment motions and redistributions. This is in contrast to the relatively little morphological variation at the solid support/polymer interface because of the constraints imposed by silyl cross-linking and the hydrophobic barrier to water diffusion. The middle part of the PC film was found to have constant scattering length density, which would indicate no structured inhomogeneity along the surface normal direction. However, a small-angle neutron scattering (SANS) study on wet 0.2 mm thick cast films suggests the formation of randomly packed anisotropic water pools of dimensions 50–100 Å, surrounded by

**Table 1. Structural Parameters for Different Monomers in PC100B Polymer**

monomer	PC <sup>b</sup>	dodecyl <sup>b</sup>	hydroxypropyl <sup>b</sup>	silyl <sup>b</sup>
mol frac	23	47	25	5
length (Å) <sup>a</sup>	20.4	24.1	12.4	13.1
width (Å) <sup>a,c</sup>	6.5	5.5	5.5	8.5
vol (Å <sup>3</sup> ) <sup>d</sup>	450	485	243	361
SLD (Å <sup>-2</sup> )	0.9 × 10 <sup>-6</sup>	0.1 × 10 <sup>-6</sup> 5.5 × 10 <sup>-6</sup> <sup>e</sup>	0.8 × 10 <sup>-6</sup>	0.7 × 10 <sup>-6</sup>

<sup>a</sup> All data were calculated by software Molecular Modeling Pro (MMP, ChemSW Inc.). <sup>b</sup> Parameters included the size of methacrylate monomer. <sup>c</sup> The maximal molecular width was used at its straight state of configuration. <sup>d</sup> Volume calculated from corrected mass density in MMP software. <sup>e</sup> SLD of deuterated dodecyl chain.

polymer matrix. Since water flows freely in to and out of these films, the pores in wet films are presumably interconnected.

## Experimental Section

**Materials.** The synthetic procedures for making PC100B (also known as PC1036) have been described in ref 35. Copolymerization of dodecyl methacrylate (LM, 47 mol %), methacryloyloxyethylphosphorylcholine (MPC, 23%), 2-hydroxypropyl methacrylate (HPM, 25%), and trimethoxysilylpropyl methacrylate (TPM, 5%) was initialized using 1% AIBN ( $\alpha,\alpha'$ -azoisobutyronitrile), and the reaction was carried out at 62 °C in ethanol. The raw polymer product was purified by double precipitation into acetone, typically yielding between 70 and 90% of a free white powder. The final product was sealed and stored at -18 °C until use. The partially deuterated polymer was made and purified in exactly the same reaction conditions. The dodecyl chain deuterated methacrylate monomer was prepared via reaction of methacryloyl chloride (98+%, Aldrich) with deuterated dodecanol (*n*-C<sub>12</sub>D<sub>25</sub>OH, 98% D from Cambridge Isotopes). The monomer was purified through silica flash column before distillation was made under inhibitor. The physical constants for the monomeric fragments of hydrogenated and partially deuterated PC100B used in the model fitting are listed in Table 1. The chemical structure of the copolymer has been given in Scheme 1 in ref 23.

**Film Preparation.** Thin PC polymer films were prepared by dip coating silicon blocks of dimensions of 2.5 × 5 × 12.5 cm<sup>3</sup> in PC polymer solutions using a specifically designed coating rig as described in ref 13. The mixture of hexane and ethanol in the volume ratio of 1:1 was used as solvent. For preparing films with thickness from 100 to 500 Å, polymer solutions at different concentrations were made. To remove possible insoluble particles, the solutions were filtered through paper filters. Varying solution concentrations together with different motor lifting speeds helped to produce films with required thickness and persistent uniformity. The coated films were dried in air for at least 2 h at ambient temperature before they were annealed at 50 and 150 °C for 3 h under vacuum. The samples were then left to cool to ambient temperature naturally and were then kept in a vacuum desiccator for subsequent characterization. Annealing helped to relax the tension confined in the polymer fragments, but for the PC polymers used in this work, a more important role was to induce silyl cross-linking, which was found to be strongly temperature dependent.<sup>23,24</sup>

Prior to the film coating, the blocks were polished using diamond emulsions with different particle sizes. The polished silicon blocks were then immersed in 1% Decon solution for 1 h to clean any residue chemicals and contaminants from the polished surfaces. Then a Piranha solution composed of 95 parts of concentrated sulfuric acid (98%) and 5 parts of hydrogen peroxide (29%) was used to clean any further organic traces on the block surface. This was administered by immersing the Si blocks in Piranha solution at 90 °C for 2 min, followed by rinsing with a large quantity of deionized water. This procedure ensured a consistent hydrophilic block surface,

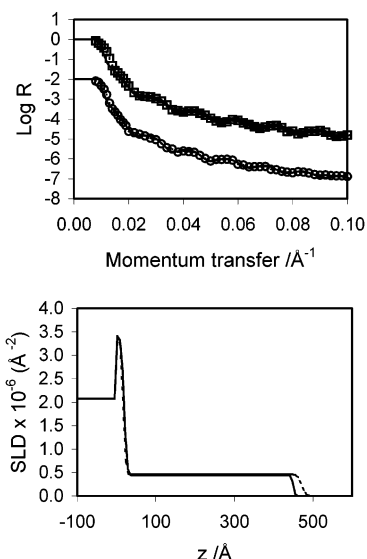


**Figure 1.** (a) Measured neutron reflectivity and calculated fits for dry PC100B films annealed at 50 °C (□) and at 150 °C (○). The data have been vertically offset for comparison. (b) Derived SLD profiles from (a) with continuous line for the film annealed at 150 °C and dotted line at 50 °C.

as indicated by the same amount of chicken egg white lysozyme adsorption at 1 g dm<sup>-3</sup> under pH 7.<sup>19</sup>

Neutron reflection measurements were done using reflectometers CRISP and SURF at the ISIS Neutron Facility, Rutherford Appleton Laboratory, UK.<sup>36</sup> Both reflectometers use white beam with wavelengths ranging from 0.5 to 6.5 Å. Their full range of momentum transfer,  $\kappa$  ( $\kappa = 4\pi \sin \theta / \lambda$ , where  $\theta$  is the beam incidence angle and  $\lambda$  is the beam wavelength), was provided by a combination of three measurements at glancing angles of 0.5°, 1°, and 1.5° at the air/solid interface and 0.35°, 0.8°, and 1.8° at the solid/solution interface. For both types of reflectivity measurements, the incoming neutron beam was directed downward toward the sample and was reflected from the interface upward and into the detector. For the measurements at the air/solid interface, the incoming and reflected beams traveled through air. For the measurements at the solid/water interface, the beam was directed into the solid/water interface from the small face of the silicon block and exited from the opposite side of the small face into the detector. The large polished face of silicon block was clamped against a Teflon cell into which D<sub>2</sub>O was injected. The dimension of the beam at a given incidence angle was defined by sets of vertical and horizontal cadmium slits. The beam width was set by the vertical slits, and its maximal value was limited by the solution width inside the trough. The height of the beam was set by the horizontal slits, and at each incidence angle care was taken not to over-illuminate the surface while optimizing the maximum beam intensity. The measured reflectivity profiles were analyzed using a model fitting routine based on optical matrix formula.<sup>37</sup>

SANS measurements were made on the LOQ beamline at ISIS, using wavelengths of 2.2–10 Å simultaneously by time-of-flight at a sample–detector distance of 4.1 m. Samples were wrapped in aluminum foil to retain water, background from an empty foil packet was subtracted, and data were corrected for wavelength-dependent sample transmission, detector efficiency, and monitor spectrum shape.

## Results and Discussion

**Structure of Dry Films.** Neutron reflectivity was first used to determine the structure of dry PC100B films coated on silicon surface. Figure 1a shows two neutron reflectivity profiles of dry PC100B films measured at the air/solid interface. The two films were annealed at 50 and 150 °C. The reflectivity curves are

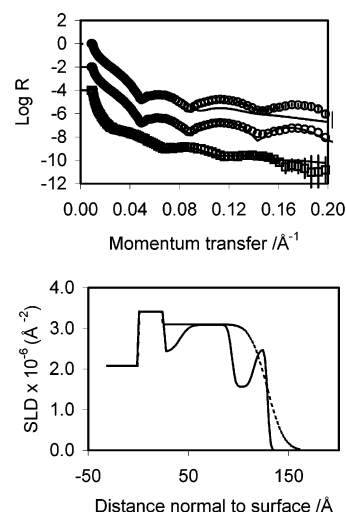


**Figure 2.** (a) Neutron reflectivity measured at the air/solid interface together with the fitted profiles (continuous lines) for the dodecyl chain deuterated dry film of a nominal dry thickness of 115 Å (○). The reflectivity from the fully hydrogenated PC100B film with a nominal dry thickness of 130 Å is shown for comparison (□). Both films were annealed at 150 °C. (b) The single- and four-layer SLD profiles corresponding to the two fits in (a) to the deuterated PC100B film. The hydrogenated polymer film fits to a uniform layer of 130 Å, with SLD not shown. In (b) the oxide layer is represented by the first square peak on the left.

vertically offset for clarity. Their overall shape is similar, indicating that annealing temperature has no major effect on the overall thickness and composition of these films. The continuous lines shown in Figure 1a were calculated using the layer modeling based on optical matrix formula,<sup>37</sup> and their corresponding scattering length density (SLD) profiles are shown in Figure 1b. The SLD profiles share the same horizontal axis, with the silicon/silicon oxide interface located at  $z = 0$  and the film in the half-space  $z > 0$ . The total film thickness was found to be 410 Å when annealed at 150 °C and 455 Å at 50 °C. A roughness of 3 Å was applied at the SiO<sub>2</sub>/polymer interface and some 15 Å at the polymer/air interface. These values were within  $\pm 20$  Å identical to the fitted results from the prior spectroscopic ellipsometry analysis.<sup>23,24</sup>

Just from the small difference of SLD between the two measurements alone, it is difficult to identify the effect of annealing on the polymer film structure. It can however be seen from Figure 1a that higher annealing temperature produces clearer oscillation fringes in the reflectivity curve, indicating that the higher temperature annealing resulted in sharper interfacial structuring. In addition, higher annealing temperature is likely to smoothen the air/polymer interface and help remove the possible voids inside the polymer matrix.<sup>23,24</sup> Because the polymers used in these reflectivity studies were fully hydrogenated, the isotopic contrasts between different segments within the polymer were relatively small. The result would therefore be well expected.

Subsequent reflectivity measurements were made using PC polymer films formed from the dodecyl chain deuterated PC100B. Figure 2a compares the reflectivity profile obtained from a partially deuterated film annealed at 150 °C with that from another film coated from the fully hydrogenated PC100B (the low profile in Figure 2a). Both films were processed under identical conditions. The SLD of the deuterated PC100B polymer is  $3 \times 10^{-6}$  Å<sup>-2</sup>, as compared with  $0.48 \times 10^{-6}$  Å<sup>-2</sup> for



the fully hydrogenated counterpart. Because of the high isotopic contrast introduced by the deuterated moiety, the whole reflectivity obtained from the partially deuterated film shown in Figure 2a shows an altered pattern, as indicated by higher reflectivity level and stronger oscillation fringes. The film thickness of the deuterated sample was found to be about 115 Å, simply from the oscillation frequency, and the corresponding thickness for the hydrogenated sample to be around 130 Å. Both values were within  $\pm 10$  Å, consistent with those derived from the earlier ellipsometric measurements.

Various layered interfacial distributions were tried, ranging from one layer to multilayer models. Obviously, the one-layer structure was not a good model to describe the reflectivity profile for the partially deuterated PC100B film, as can be seen from comparison of the best one layer fit with the measured reflectivity shown in Figure 2a. A range of combinations with layered models with alternate SLD were subsequently tested, and it is clear that the models providing appropriate fits had to start with a lower SLD layer of some 10 Å adjacent to the SiO<sub>2</sub> surface. This was followed by a higher SLD layer of some 30 Å, further followed by a second lower SLD of about 15 Å. In all cases, a thin layer of some 20 Å with higher SLD at the outer polymer/air interface was found to be essential to generate the right interference fringe. It is also useful to mention that models with the opposite order of the SLD alteration were found not to fit the measured reflectivity well. Because the SLD for dodecyl methacrylate bearing the deuterated dodecyl group is  $5.32 \times 10^{-6} \text{ Å}^{-2}$  and the rest of the PC100B polymer has the SLD of  $1.15 \times 10^{-6} \text{ Å}^{-2}$ , it is clear that the layers having the lower SLD mainly contain hydrophilic segments including 2-hydroxypropyl groups and PC groups and that the layers having the higher SLD largely contain the hydrophobic dodecyl chains. Thus, the marked structural feature in the ultrathin PC 100B films is the formation of layered structure arising from component segregation near the air/polymer and polymer/substrate interfaces.

Segregation is expected to occur during polymer annealing or melting and has indeed been observed at the surfaces and interfaces of multicomponent polymers, including polymer blends,<sup>38,39</sup> polymers with functional end groups,<sup>40</sup> and block copolymers.<sup>41–43</sup> The driving forces governing this behavior are the differences in surface energy between the mixed components<sup>30</sup> and the affinities of the components toward the substrate surface. In addition, the isotopic effect is also one of the possible contributions; the deuterated component might preferentially segregate to the air/polymer and polymer/substrate interfaces.<sup>29</sup> The segregation of deuterated component occurs due to a weakly unfavorable  $\chi$  interaction parameter originating from the difference in polarizability between C–H and C–D bonds.<sup>44</sup> This is likely to cause possible difference between the fully hydrogenated and partially deuterated PC polymer pair, but the main structural feature of segregation is expected to hold for such a polymeric system.

The formation of an outer layer of some 20 Å at the polymer/air interface may arise from the alkyl chain enrichment upon annealing. In contrast, the formation of a hydrophilic thin layer of 10–20 Å closest to the SiO<sub>2</sub> surface is consistent with the possible enrichment of trimethoxysilane groups (TMS) in this region, driven by the silyl cross-linking between TMS groups and the hydroxy groups on SiO<sub>2</sub> surface.<sup>45</sup> This thin hydrophilic

layer is immediately followed by a thicker layer of some 30 Å with higher SLD, indicating the presence of hydrophobic dodecyl chains. The subsequent repeat of this alternate layered pattern is most likely to be induced by the preferential segregation of the first two layers.

It is also interesting to note that when the best four-layer model was used (with its SLD shown as continuous line in Figure 2b), the SLD for the outer layer is about  $2.5 \times 10^{-6} \text{ Å}^{-2}$ , as compared with  $3.3 \times 10^{-6} \text{ Å}^{-2}$  obtained for the middle hydrophobic layer. It is possible that the difference simply indicates the mixing of some hydrophilic moieties due to the energy balance and the polymer chain confinement. An alternative explanation is the possible penetration of moisture from air, resulting in a reduced SLD value. If the average SLD for the dry state is assumed to be  $3 \times 10^{-6} \text{ Å}^{-2}$  and that for the wet state is  $2 \times 10^{-6} \text{ Å}^{-2}$ , the volume fraction of water ( $\phi_{\text{water}}$ ) can be estimated from the following expression

$$\rho_0 = \rho_{\text{water}}\phi_{\text{water}} + (1 - \phi_{\text{water}})\rho_{\text{polymer}} \quad (1)$$

where  $\rho_0$  is the measured SLD of outside layer;  $\rho_{\text{water}}$  and  $\rho_{\text{polymer}}$  represent the SLDs for water and deuterated PC100B, respectively. The input of the SLDs into eq 1 gave a value of ca. 0.3 for  $\phi_{\text{water}}$ . Absorption of this level of water into the outer surface region could cause uneven swelling and disrupt the uniformity of the outer film surface. This appears to be consistent with the need of a roughness of some 10 Å to describe the segment distribution on the outer surface. Note that water uptake from open air into freshly annealed PC polymer films was often revealed from the SLD changes over the outer film surface. As a result, freshly annealed films needed to be stored in dry nitrogen protected environment.

As already shown in Figure 1, the best fit to the hydrogenated polymer film in Figure 2a approximates to a uniform layer of ca. 130 Å. Although it does not provide much detailed information inside the film, it also shows the requirement of the roughness of some 15 Å on the outer polymer surface, further confirming the structural deterioration caused by moisture absorption. The agreement of the extent of roughening of the outer polymer surfaces tends to suggest that the hydrogenated and deuterated PC100B polymers have similar film structure.

**Structure of Swollen Films.** Our previous ellipsometric data have already shown that PC 100B films can absorb some 30–60% water, depending on the annealing temperature.<sup>23,24</sup> The neutron reflectivity data described above suggest implicitly the formation of a layered structure within the dry polymer films. It is interesting to find out how such a layered structure varies once exposed to water. It is particularly useful to follow the possible structural change of the outer surface layer which contains a relatively high content of hydrophobic dodecyl chains.

Figure 3 shows the neutron reflectivity measured at the silicon oxide/D<sub>2</sub>O interface and the fitted SLD profiles for a PC100B film with the nominal dry thickness of 430 Å annealed at 150 °C. To compare the effect of annealing, Figure 4 presents the same data for another PC film with the nominal dry thickness of 450 Å but annealed at 50 °C. It can be seen from Figures 3a and 4a that the frequency of oscillations in the reflectivity of the PC100B film annealed at 50 °C is

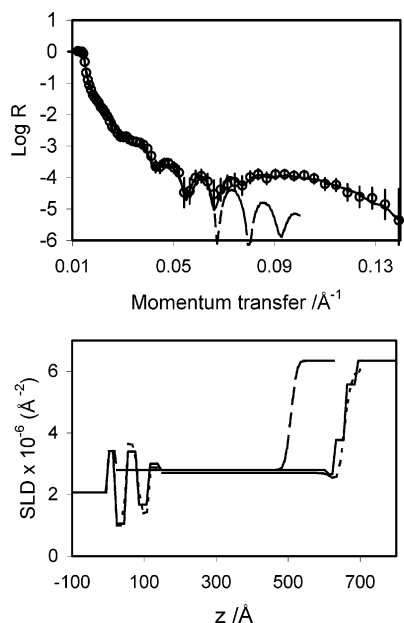


**Figure 3.** (a) Neutron reflectivity measured at the solid/D<sub>2</sub>O interface for a PC100B film with nominal dry thickness of 430 Å annealed at 150 °C. The long dashed line represents a single uniform layer fit; the short dashed line representing a multiple layer model fitting with a roughness of ca. 50 Å on the outer surface and the continuous line representing the same fit but using a step function to model the outer polymer surface appear to be identical. (b) Derived SLD profiles from (a) with the first square peak on the left representing the oxide layer.

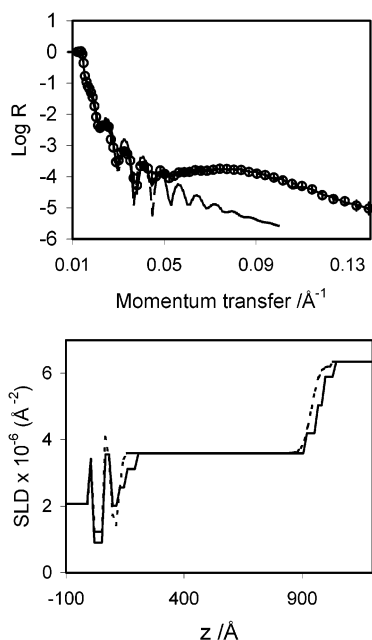


**Figure 4.** (a) Neutron reflectivity measured at the solid/D<sub>2</sub>O interface for a PC100B film with nominal dry thickness of 455 Å annealed at 50 °C. The short dashed line representing a multiple layer model fitting with a roughness of ca. 50 Å on the outer surface and the continuous line representing the same fit but using a step function to model the outer polymer surface produce identical reflectivity fits. (b) Derived SLD profiles from (a) with the first square peak on the left representing oxide layer. The SLD corresponding to the reflectivity calculated from the best single uniform layer fit (long dashed line in (a)) was not shown in (b) for clarity.

greater, indicating a thicker film after hydration. This observation is entirely consistent with our previous ellipsometry results, showing that films annealed at the

lower temperature take up more water and become thicker. Each of the reflectivity curves shows a broad bump between 0.06 and 0.1 Å<sup>-1</sup>, which implies some common features in their swollen structure. The dashed lines in Figures 3a and 4a represent the best one-layer fits, which clearly do not fit the measured reflectivity profiles over the high  $\kappa$  range, although they do fit the measured reflectivities well over the low  $\kappa$  range (e.g., from 0.01 to 0.05 Å<sup>-1</sup>). This suggests that the single-layer model only reflects part of the film structural features. As in the case of dry films, models with more than one layer were subsequently tested. Those that fit the measured reflectivities exhibited pronounced oscillations near silicon oxide surface. These oscillations dampened out as the profiles propagated into the interior of the films. Meanwhile, layers with higher water content were found at the water/polymer interface. The fitting analysis showed that the models with segregated layers were the only structure to describe the large bumps appeared in the measured reflectivities. It should be mentioned at this point that oscillatory concentration–depth profiles have been predicted and observed for a number of copolymer systems.<sup>40,46,47</sup>

As already shown previously, the oscillatory structure was not easily detected in dry hydrogenated PC100B films, but penetration of D<sub>2</sub>O substantially enhanced the isotopic contrast. Thus, the first question to be answered is whether water swelling just simply expands the dry PC100B film thickness, or it causes further structural alterations. Figures 3b and 4b show that the first layer on the SiO<sub>2</sub> surface has a low SLD layer and is about some 30 Å thick. This would mean a low water content and hence a hydrophobic layer in the region adjacent to the surface of hydrophilic silicon oxide. We had anticipated, on the basis of surface energy, that the zwitterionic PC groups, 2-hydroxypropyl groups, and silyl cross-linking segments be enriched preferentially on the SiO<sub>2</sub> surface, as discussed previously. The possible answer is that this hydrophilic layer is very thin and tightly confined and that its SLD in the presence of D<sub>2</sub>O must be either between that of SiO<sub>2</sub> and that of the hydrophobic layer or close to one of the two. The combination of these features means that its existence does not have a strong influence on the overall reflectivity. Indeed, if this thin layer was inserted into the calculation of reflectivity, it had little observable effect over the entire reflectivity profile. This explains why this layer was not detected in the initial modeling based on the criterion of the use of a minimal number of layers and parameters in the fitting process. In contrast, the presence of the first hydrophobic layer was easily detected from the modeling.

The inner 30 Å hydrophobic layer is immediately followed by a hydrophilic region mainly consisting of PC groups and 2-hydroxypropyl groups, with its thickness around 35 Å. This hydrophilic layer is in turn followed by a further hydrophobic layer, but the thickness of this layer is about 25 Å for the film annealed at 150 °C (Figure 3b), 35 Å for that annealed at 50 °C (Figure 4b). Beyond this interfacial segregation the measured reflectivities do not justify any further adoption of an oscillatory SLD profile, and the middle region of the films is well represented by a constant SLD. As can be seen from Figures 3b and 4b, the uniform middle region spans some 500 Å and occupies the main body of the films. The water content in this region is 40% for the film annealed at 150 °C and 55% for the film annealed

at 50 °C. The variation in the equilibrated water content clearly reflects the effect of annealing temperature on the extent of silyl cross-linking. The uniform structural feature of the middle film region explains why one layer model could approximately fit the main part of the measured reflectivities. This observation is consistent with our previous ellipsometric measurements.

Although the layered structural features at the solid/polymer interface have substantial influence on the shape of reflectivity profiles, it is the structural feature at the polymer/water interface that is directly relevant to its protein repellent behavior. As shown in Figures 3b and 4b, we have first attempted to model the outer swollen film surfaces with several step layers, with the total thickness for this region spanning over 100 Å. This gradual change in the volume fraction of the polymer segments can also be described using roughness. Both treatments reflect the feature of high water content over a wide interfacial region. For example, over the outermost layer of some 30 Å, there was some 80% water in the film annealed at 150 °C and over 90% in the film annealed at 50 °C, implying that some polymer chains or loops are dangling over the outer polymer surfaces. It is interesting to note that there is a small but detectable layer near the outer surface of the polymer film annealed at 150 °C with a low scattering length density. This layer was transient in the course of film swelling and was not observed in the polymer film annealed at 50 °C, possibly because of the loose cross-linking. It should be recalled that structural determination of deuterated PC100B film (Figure 2b) clearly revealed a hydrophobic layer on the outer surface of the dry PC100B polymer film, arising from surface energy minimization. This together with the results shown in Figure 3b suggests that upon swelling substantial structural rearrangement has occurred. Swelling associated with segment rearrangement has drastically altered the confined structure on the outer surfaces of the polymer films, resulting in the preferential expression of hydrophilic segments toward the bulk water.

It can thus be said that, in light of the layered structure observed for the dry PC films, swelling has substantially altered the outer surface film structure. This is in contrast to the layered structure feature that has been largely retained in the inner part of the PC films. For films annealed at both annealing temperatures, the layered structure at the SiO<sub>2</sub>/polymer interface spans across some 100 Å, and there is no significant structural variation with annealing temperature. In fact, the whole segregated region of about 100 Å is almost comparable to that probed for the dry films (see Figure 2). However, the overall expansibility (defined as the ratio of total swollen film thickness to the dry film thickness) showed a strong dependency on annealing temperature. The overall expansibility is 1.6 for PC polymer films annealed at 150 °C and 2.8 for those annealed at 50 °C. Thus, the swelling must arise mainly from the expansion of the middle and outer film surface regions. While it is difficult to quantify various effects imposed on the swelling of the inner segregated region, the silyl network and the hydrophobic sublayers must be the two main constraining key factors.

To examine the effect of dry film thickness on structural segregation, neutron reflectivity was also used to determine the structure of a fully hydrogenated PC 100B film with a dry film thickness of 140 Å, also annealed at 150 °C (Figure 5). Data analysis showed

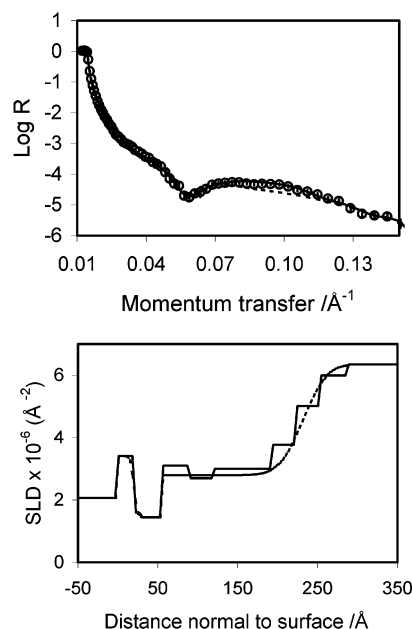


**Figure 5.** (a) Neutron reflectivity measured at the solid/D<sub>2</sub>O interface for a PC100B film with nominal dry thickness of 140 Å annealed at 150 °C. Dashed line represents a multiple layer model fitting with a roughness of ca. 50 Å on the outer surface; continuous line represents the same fit but using a step function to model the outer polymer surface. (b) Derived SLD profiles from (a) with the first square peak on the left representing the oxide layer.

that the overall dimension of the layer was again dominated by a broad middle region that was well described by a uniform layer model. A thin inner layer of some 10 Å with SLD of  $2 \times 10^{-6} \text{ Å}^{-2}$  was detected near the silicon oxide surface. On top of this hydrophilic layer was the hydrophobic layer of ca. 30 Å thick with its SLD of  $1.2 \times 10^{-6} \text{ Å}^{-2}$ , indicating the formation of the hydrophobic region. At least two further sublayers were required to fit the main shape of the interference fringes in the reflectivity, thus further confirming the oscillatory SLD feature at the solid/polymer interface. A further common feature was the diffuse outer film surface at the polymer/water interface, which was well described by a multistep layer profile. Thus, the key structural feature for both thin and thick films are the same and change in dry film thickness only affects the dimension of the uniform middle layer region.

To ascertain the main findings described above, neutron reflection measurement was also made to the film formed from the dodecyl chain deuterated PC 100B polymer in D<sub>2</sub>O. The dry film was about 120 Å thick and annealed at 150 °C. Figure 6a shows the measured reflectivity at the solid/D<sub>2</sub>O interface together with the best fits, and Figure 6b shows the derived SLD profiles. Two models were used to fit the measured reflectivity profile and both produced comparable quality of fits. This result was well expected because the only difference between them was the description of the diffuse outer surface. Unlike the fully hydrogenated polymer films in D<sub>2</sub>O, no oscillatory SLD profile was detected at the SiO<sub>2</sub>/polymer interface. Hence, the main finding from the analysis of this reflectivity profile is the uniform SLD throughout the main body of the film. In comparison with the situation for the fully hydrogenated PC100B films, the deuterated dodecyl segments have a high SLD, and the SLD for the hydrophobic sublayers is around  $(3\text{--}4) \times 10^{-6} \text{ Å}^{-2}$ . At the same time, the



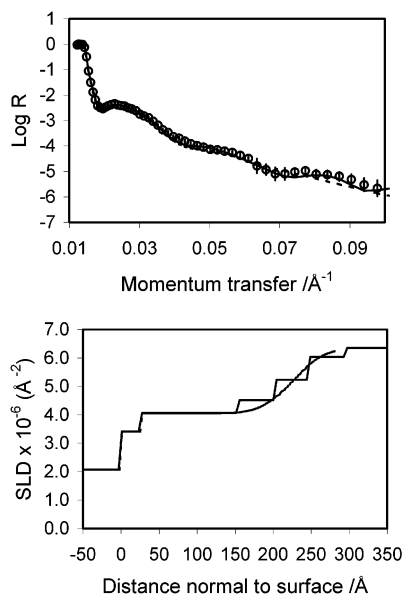


**Figure 6.** (a) Neutron reflectivity measured at the solid/D<sub>2</sub>O interface for a deuterated PC100B film with nominal thickness of 100 Å annealed at 150 °C. Dashed line represents a multiple layer model fitting with a roughness of ca. 50 Å on the outer surface; continuous line represents the same fit but using a step function to model the outer polymer surface. (b) Derived SLD profiles from (a) with the first layer on the left representing oxide layer.

hydration of D<sub>2</sub>O into the hydrophilic sublayers brings their SLD values to the similar value. The total effect is the reduced difference in SLD between hydrophilic and hydrophobic sublayers, resulting in an almost uniform layer distribution. Thus, the result from the partially deuterated PC 100B film in D<sub>2</sub>O is entirely consistent with the main structural features revealed from the fully hydrogenated films.

The neutron reflection results described above have shown similar layered structural features at the SiO<sub>2</sub>/polymer and polymer/water interfaces, and that change in the PC film thickness appears to alter the middle part of the polymer film represented by a constant SLD profile. However, constant SLD does not rule out the possible formation of isotropically structured topology inside the film.

Small-angle neutron scattering (SANS) is effective at revealing any possible structural details under submicron dimension. To reduce surface effects and optimize the signal contribution from the main body of the film, free films of PC 100B of thickness of 0.2–0.3 mm were studied. One film was studied as prepared from evaporation of an ethanol/hexane solution using SANS, while another was cured under  $\gamma$  irradiation, equivalent to thermal annealing at 150 °C.<sup>48</sup> Dry films showed no significant scattering, indicating no air filled pores were present. Films swollen in D<sub>2</sub>O showed strong scattering, which was very similar for both the irradiated (cross-linked) and as-prepared samples. Figure 7 compares the scattering profile measured from the irradiated film with the best fit. The strong peak at  $\kappa \sim 0.065 \text{ Å}^{-1}$  indicates a characteristic spacing of around 100 Å. After consideration of a number of simple model fits the data seem to be most consistent with a form factor  $P(\kappa)$  for randomly oriented prolate ellipsoids (minor radius  $\sim 27 \text{ Å}$ , axial ratio  $\sim 2.0$ ) combined with a hard sphere (noninteracting) form factor  $S(\kappa)$  for a volume fraction around 0.22 and radius 38 Å. The absolute intensities

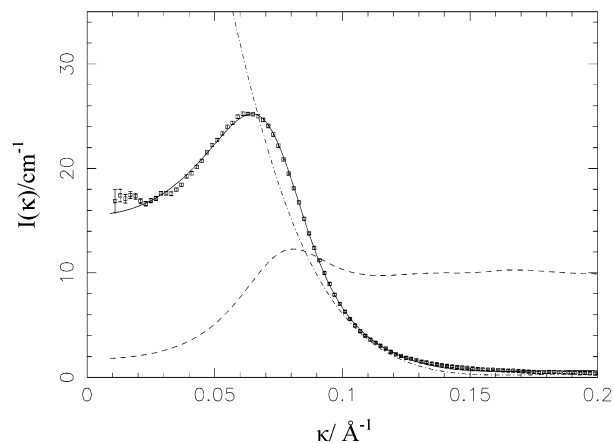


**Figure 7.** SANS intensity ( $I(\kappa)/\text{cm}^{-1}$ ) from bulk PC 100B film swollen with D<sub>2</sub>O. A form factor  $P(\kappa)$  for monodisperse ellipsoids, diameter  $\sim 50 \text{ Å}$ , length  $\sim 100 \text{ Å}$  (dot-dashed), is combined with a hard-sphere structure factor  $S(\kappa)$  (shown dashed  $\times 10$ ) to give the overall fit (solid line). This suggests a network of anisotropic water pools throughout the bulk of the transparent gel.

and shape of the scattering are then fairly consistent with a 15–20% volume fraction of anisotropic (rather than spherical) water pools set in a polymer matrix. The fact that water flows freely in to and out of the films suggests that these pools are connected by smaller channels. Unfortunately, there was insufficient material available to collect SANS from a deuterated polymer, for which a dry sample should give a SANS signal on the hypothesis that hydrophilic regions have phase separated in the center of the films into a droplet network rather than a lamellar structure. Further SANS experiments are planned to investigate the possibility of controlling the shape and size of the pores with annealing conditions and polymer composition.

## Conclusions

We outline the main structural features obtained from the PC polymer films using schematic representation as depicted in Figure 8. We summarize the main observations in three different film regions. For simplicity, the schematic models only give considerations on the relative effects of hydrophilic and hydrophobic moieties before and after swelling.

Figure 8a shows that while the dry outer surface region is well represented by a layered structure feature, swelling causes major structural disruption, resulting in uneven polymer fragment distribution. The swelling is also likely to cause the preferential exposure of the zwitterionic PC groups to the bulk aqueous phase, enabling the polymeric film surface to reduce protein adsorption as effectively as self-assembled monolayer bearing terminal PC groups.<sup>15</sup> The enrichment of hydrophobic moieties on the outer surface of dry PC polymer films has also been observed by angle-resolved XPS and ToF-SIMS by Clarke et al.<sup>49</sup> By performing dynamic contact angle (DCA) measurements, these authors have also demonstrated the force variations characteristic of hydrophobic and hydrophilic surfaces corresponding to dry and wetted film surfaces, indicating the possible preferential expression of different segments driven by surface energy minimization. These observations are in strong support of the structural details revealed by NR.

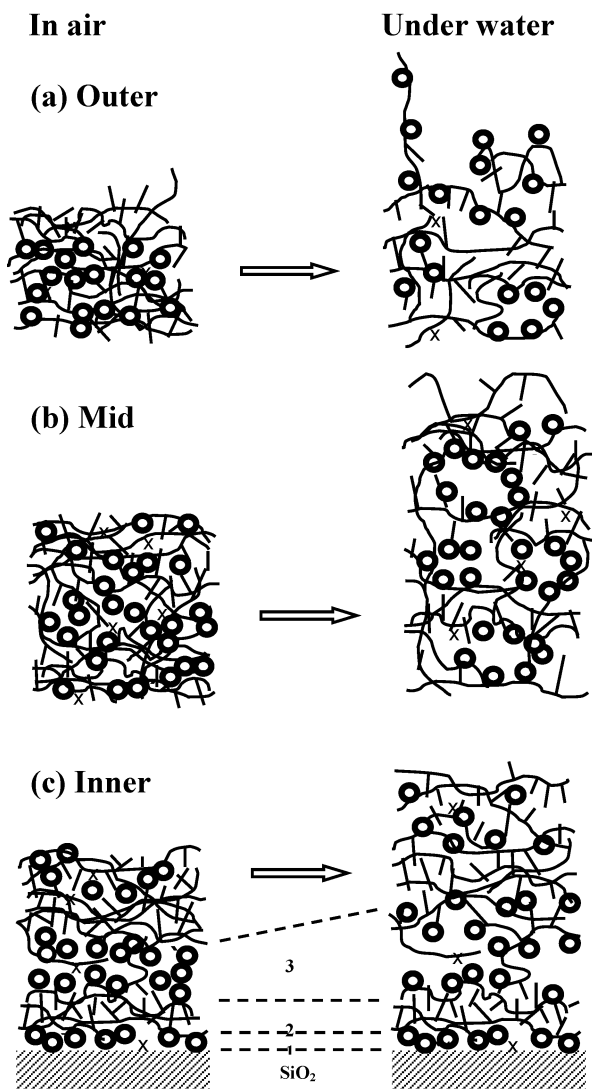


**Figure 8.** Schematic representation of film structural changes (a) at outer polymer surface, (b) in the middle region of the polymer film, and (c) at the  $\text{SiO}_2$ /polymer interface before (left) and after (right) swelling. In graph (c) layer 1 represents a hydrophilic layer on top of  $\text{SiO}_2$  with a thickness about 10 Å, and layer 2 represents a hydrophobic layer with a thickness 20 Å, followed by a hydrophilic layer (layer 3) with a swollen thickness of 30–40 Å. The circles represent hydrophilic entities, and lines represent polymer matrices.

Figure 8b depicts the film thickness expansion for the middle region before and after swelling. While neutron reflectivity showed constant SLD across the region, indicating no structural alignment along the surface normal direction, SANS revealed formation of nanoporous network with anisotropic water pores of around 50 Å in diameter. The middle film region represents the main water uptake.

Figure 8c outlines the oscillatory layering feature at the  $\text{SiO}_2$ /polymer interface. Neutron reflectivity indicates the requirement of a minimum of four sublayers starting with the thin hydrophilic layer of some 10 Å closest to the hydrophilic  $\text{SiO}_2$ , followed by a hydrophobic 30 Å layer, and then followed by further hydrophilic and hydrophobic layers of 20–30 Å each. In comparison to the other parts of the film regions, water penetration does not cause any significant expansion in its thickness, although water association with the hydrophilic sublayers was clearly indicated by a shift in SLD.

**Acknowledgment.** We thank Biological and Biotechnological Sciences Research Council (BBSRC) and Engineering and Physical Sciences Research Council (EPSRC) for support. Y. Tang thanks Biocompatibles Ltd. for financial support and the British government for an Overseas Research Studentship (ORS).

## References and Notes

- (1) Andrade, J. D. *Surface and Interfacial Aspects of Biomedical Polymers*; Plenum: New York, 1988; Vol. 2.
- (2) Andrade, J. D.; Hlady, V. *Adv. Polym. Sci.* **1986**, *79*, 1.
- (3) Chapman, R. G.; Ostuni, E.; Yan, L.; Whitesides, G. M. *Langmuir* **2000**, *16*, 6927.
- (4) Chapman, R. G.; Ostuni, E.; Liang, M. N.; Meluleni, G.; Kim, E.; Yan, L.; Pier, G.; Warren, H. S.; Whitesides, G. M. *Langmuir* **2001**, *17*, 1225.
- (5) Ostuni, E.; Chen, C. S.; Ingber, D. E.; Whitesides, G. M. *Langmuir* **2001**, *17*, 2828.
- (6) Ostuni, E.; Chapman, R. G.; Liang, M. N.; Meluleni, G.; Pier, G.; Ingber, D. E.; Whitesides, G. M. *Langmuir* **2001**, *17*, 6336.
- (7) Ostuni, E.; Chapman, R. G.; Holmlin, R. E.; Takayama, S.; Whitesides, G. M. *Langmuir* **2001**, *17*, 5605.
- (8) Holmlin, R. E.; Chen, X.; Chapman, R. G.; Takayama, S.; Whitesides, G. M. *Langmuir* **2001**, *17*, 2841.
- (9) McPherson, T.; Kidane, A.; Szleifer, I.; Park, K. *Langmuir* **1998**, *14*, 176.
- (10) Jenny, C. R.; Anderson, J. M. *J. Biomed. Mater. Res.* **1999**, *44*, 206.
- (11) Rabinow, B. E.; Ding, Y. S.; Qin, C.; McHalsky, M. L.; Schneider, J. H.; Ashline, K. A.; Shelbourn, T. L.; Albrecht, R. M. *J. Biomater. Sci., Polym. Ed.* **1994**, *6*, 91.
- (12) Brink, C.; Osterberg, E.; Holmberg, K.; Tiberg, F. *Colloids Surf.* **1992**, *66*, 149.
- (13) Murphy, E.; Keddle, J. L.; Lu, J. R.; Brewer, J.; Russell, J. *Biomaterials* **1999**, *20*, 1501.
- (14) Murphy, E.; Lu, J. R.; Brewer, J.; Russell, J.; Penfold, J. *Langmuir* **1999**, *15*, 1313.
- (15) Lu, J. R.; Murphy, E. F.; Su, T. J.; Lewis, A. L.; Stratford, P. W.; Satija, S. K. *Langmuir* **2001**, *17*, 3382.
- (16) Murphy, E. F.; Lu, J. R.; Brewer, J.; Russell, J. *Macromolecules* **2000**, *33*, 4545.
- (17) Su, T. J.; Lu, J. R.; Thomas, R. K.; Cui, Z. F. *J. Phys. Chem. B* **1999**, *103*, 3727.
- (18) Su, T. J.; Lu, J. R.; Thomas, R. K.; Cui, Z. F.; Penfold, J. *J. Phys. Chem. B* **1998**, *102*, 8100.
- (19) Su, T. J.; Lu, J. R.; Thomas, R. K.; Cui, Z. F.; Penfold, J. *Langmuir* **1998**, *14*, 438.
- (20) Su, T. J.; Lu, J. R.; Thomas, R. K.; Cui, Z. F.; Penfold, J. *J. Colloid Interface Sci.* **1998**, *203*, 419.
- (21) Lu, J. R.; Su, T. J.; Thomas, R. K.; Rennie, A. R.; Cubit, R. J. *Colloid Interface Sci.* **1998**, *206*, 212.
- (22) Su, T. J.; Green, R. J.; Wang, Y.; Murphy, E. F.; Lu, J. R.; Ivkov, R.; Satija, S. K. *Langmuir* **2000**, *16*, 4999.
- (23) Tang, Y.; Lu, J. R.; Lewis, A. L.; Vick, T. A.; Stratford, P. W. *Macromolecules* **2002**, *35*, 3955.
- (24) Tang, Y.; Lu, J. R.; Lewis, A. L.; Vick, T. A.; Stratford, P. W. *Macromolecules* **2001**, *34*, 8768.
- (25) Hayward, J.; Chapman, D. *Biomaterials* **1984**, *5*, 135.
- (26) Hayward, J.; Durrani, A.; Shelton, C.; Lee, D.; Chapman, D. *Biomaterials* **1986**, *7*, 126.
- (27) Campbell, E. J.; O'Byrne, V.; Stratford, P. W.; Quirk, I.; Vick, T. A.; Wiles, M. C.; Yianni, Y. P. *ASAIO J.* **1994**, *40*, M853.
- (28) Yianni, Y. P. In *Structural and Dynamic Properties of Lipids and Membranes*; Quinn, P. J., Cherry, R. J., Eds.; Portland Press: New York, 1992.
- (29) Bucknall, D. G. In *Modern Techniques for Polymer Characterisation*; Pethrick, R. A., Dawkins, J. V., Eds.; Wiley: Chichester, 1999.
- (30) Jones, R. A. L.; Richards, R. *Polymers at Surfaces and Interfaces*; Cambridge University Press: New York, 1999.
- (31) Geoghegan, M.; Jones, R. A. L.; Payne, R. S.; Sakellariou, P.; Clough, A. S.; Penfold, J. *Polymer* **1994**, *35*, 2019.
- (32) Levicky, R.; Knoeripalli, N.; Tirrell, M.; Ankner, J. F.; Kaiser, H.; Satija, S. K. *Macromolecules* **1998**, *31*, 4908.
- (33) Yim, H.; Kent, M.; McNamara, W. F.; Ivkov, R.; Satija, S.; Majewski, J. *Macromolecules* **1999**, *32*, 7932.
- (34) Zhulina, E. B.; Halperin, A. *Macromolecules* **1992**, *25*, 5730.
- (35) Lewis, A. L.; Cumming, Z. L.; Goreish, H. C.; Kirkwood, L. C.; Tolhurst, L. A.; Stratford, P. W. *Biomaterials* **2001**, *22*, 99.



- (36) Penfold, J.; Richardson, R. M.; Zarbakhsh, A.; Webster, J. W. P.; Bucknall, D. G.; Rennie, A. R.; et al. *J. Chem. Soc., Faraday Trans.* **1997**, *93*, 3899.
- (37) Born, M.; Wolf, E. *Principles of Optics*; University Press: Cambridge, 1997.
- (38) Pan, D. H.; Prest, M. W., Jr. *J. Appl. Phys.* **1985**, *58*, 15.
- (39) Bhatia, Q. S.; Pan, D. H.; Koberstein, J. T. *Macromolecules* **1988**, *21*, 2166.
- (40) Elman, J. F.; Johs, B. D.; Long, T. E.; Koberstein, J. T. *Macromolecules* **1994**, *27*, 5341.
- (41) Rastogi, A. K.; St. Pierre, L. E. *J. Colloid Interface Sci.* **1969**, *31*, 168.
- (42) Bucknall, D. G.; Higgins, J. S.; Penfold, J.; Rostami, S. *Polymer* **1993**, *34*, 451.
- (43) Shull, K. R.; Winney, K. I.; Thomas, E. L.; Kramer, E. J. *Macromolecules* **1991**, *24*, 2748.
- (44) Jones, R. A. L.; Kramer, E. J.; Rafailovich, M. H.; Sokolov, J.; Schwarz, S. A. *Phys. Rev. Lett.* **1989**, *62*, 280.
- (45) Keddie, J. L.; Giannelis, E. P. *J. Am. Ceram. Soc.* **1990**, *73*, 3106.
- (46) Anastasiadis, S. H.; Russell, T. P.; Satija, S. K.; Majkrzak, C. F. *Phys. Rev. Lett.* **1989**, *62*, 1852.
- (47) Mendelle, A.; Russell, T. P.; Anastasiadis, S. H.; Satija, S. K.; Majkrzak, C. F. *Phys. Rev. Lett.* **1992**, *68*, 67.
- (48) Tang, Y. Ph.D. Thesis, University of Surrey, 2000.
- (49) Clarke, S.; Davies, M. C.; Roberts, C. J.; Tendler, S. J. B.; Williams, P. M.; O'Byrne, V.; Lewis, A. L.; Russell, J. C. *Langmuir* **2000**, *16*, 5116.

MA034647Q